Mitochondria-Targeted Nitroxide, Mito-CP, Suppresses Medullary Thyroid Carcinoma Cell Survival In Vitro and In Vivo

Dmytro Starenki and Jong-In Park

Department of Biochemistry, Medical College of Wisconsin, Milwaukee, Wisconsin 53226

Context: Medullary thyroid carcinoma (MTC) is a neuroendocrine tumor mainly caused by mutations in the *RET* proto-oncogene. For MTC therapy, the U.S. Food and Drug Administration recently approved vandetanib and cabozantinib, multikinase inhibitors targeting RET and other tyrosine kinase receptors of vascular endothelial growth factor, epidermal growth factor, or hepatocyte growth factor. Nevertheless, not all patients with the progressive MTC respond to these drugs, requiring the development of additional therapeutic modalities that have distinct activity.

Objective: We aimed to evaluate mitochondria-targeted carboxy-proxyl (Mito-CP), a mitochondria-targeted redox-sensitive agent, for its tumor-suppressive efficacy against MTC.

Design: In vitro cultures of 2 human MTC cell lines, TT and MZ-CRC-1, and TT xenografts in mice were treated with Mito-CP in comparison with vandetanib. The effects on cell survival/death, RET expression, mitochondrial integrity, and oxidative stress were determined.

Results: Contrary to vandetanib, Mito-CP induced RET downregulation and strong cytotoxic effects in both cell lines in vitro, including caspase-dependent apoptosis. These effects were accompanied by mitochondrial membrane depolarization, decreased oxygen consumption, and increased oxidative stress in cells. Intriguingly, Mito-CP–induced cell death, but not RET downregulation, was partially inhibited by the reactive oxygen species scavenger, *N*-acetyl-cysteine, indicating that Mito-CP mediates tumor-suppressive effects via redox-dependent as well as redox-independent mechanisms. Orally administered Mito-CP effectively suppressed TT xenografts in mice, with an efficacy comparable to vandetanib and relatively low toxicity to animals.

Conclusion: Our results suggest that Mito-CP can effectively suppress MTC cell growth/survival via a mechanism distinct from vandetanib effects. Mitochondrial targeting may be a potential strategy for MTC therapy. **(*J Clin Endocrinol Metab* 98: 1529–1540, 2013)**

Medullary thyroid carcinoma (MTC) is a neoplasm of the endocrine system, which originates from parafollicular C-cells of the thyroid gland (1). MTC occurs either sporadically or in hereditary forms, ie, familial MTC and multiple endocrine neoplasia (MEN) type 2 syndrome. The proto-oncogene, rearranged during transfection (*RET*), encodes a receptor tyrosine kinase whose alterations are mainly etiological to the development of MTC, although other mutations (eg, Ras mutations) are also detected in MTC at lower frequencies (2–4). For example, various mutations in the cell surface receptor domain or the cytoplasmic kinase domain constitutively activate RET in about 95% of hereditary MTC and about 50% of sporadic MTC cases (reviewed in Ref. 5). Particularly, *RET* mutations in the extracellular cysteine-rich receptor domain are mainly detected in MEN type 2A and

ISSN Print 0021-972X ISSN Online 1945-7197
Printed in U.S.A.

Received October 19, 2012. Accepted February 19, 2013.
First Published Online March 18, 2013

Abbreviations: Bcl-2, B-cell lymphoma 2; Bcl-xL, B-cell lymphoma-extra large; carboxy-H_2DCFDA, 5-(and-6)-carboxy-2′,7′-dichlorodihydrofluorescein diacetate; CGRP, calcitonin gene-related peptide; DMSO, dimethylsulfoxide; FBS, fetal bovine serum; FITC, fluorescein isothiocyanate; GAPDH, glyceraldehyde-3-phosphate dehydrogenase; MEN, multiple endocrine neoplasia; Mito-CP, mitochondria-targeted carboxy-proxyl; MTC, medullary thyroid carcinoma; NAC, *N*-acetyl-cysteine; PARP, poly(ADP-ribose) polymerase; RET, rearranged during transfection; ROS, reactive oxygen species; TMRE, tetramethyl-rhodamine ethyl ester perchlorate; TPP, triphenylphosphonium.

familial MTC, whereas its mutations in the intracellular tyrosine kinase domain are mainly detected in MEN type 2B and sporadic MTC (5). Accordingly, RET is a key primary therapeutic target in MTC. MTC is relatively rare, accounting for approximately 5% of all thyroid cancers, and progresses slowly. Nevertheless, MTC can be fatal, and the only curative therapy is surgical resection, which is not effective for metastatic or recurring MTC. The U.S. Food and Drug Administration recently approved vandetanib (trade name Caprelsa, AstraZeneca) and cabozantinib (Exelixis), multikinase inhibitors targeting RET and other tyrosine kinase receptors activated by vascular endothelial growth factor, epidermal growth factor, or hepatocyte growth factor for the treatment of inoperable progressive MTC (6, 7). Nevertheless, not all patients respond to these drugs, requiring the development of additional therapeutic strategies (6–8).

It is now well understood that mitochondrial metabolism is often reprogrammed to facilitate proliferation and survival of tumor cells. For example, mitochondrial oxidative phosphorylation in cancer is critical to meet increased demands for the production of building blocks required for uncontrolled tumor cell proliferation (reviewed in Ref. 9). Moreover, altered levels of certain metabolic byproducts from the mitochondria, such as reactive oxygen species (ROS), have been implicated in tumor initiation and maintenance as well as suppression (10–12). Accordingly, designing a rational therapeutic strategy has been attempted to exploit altered mitochondrial metabolism in cancer (13). Of note, targeting different bioactive molecules to mitochondria using the lipophilic cation, triphenylphosphonium (TPP), could effectively interfere with mitochondrial bioenergetics and suppress growth of different tumor cell lines (14). Covalent conjugation by TPP enables specific mitochondrial accumulation of a molecule via the mitochondrial membrane potential ($\Delta\psi_m$), and TPP-conjugated antioxidants have been evaluated for therapeutic purposes, mainly targeting neurodegenerative disorders (reviewed in Refs. 15 and 16). Depending upon $\Delta\psi_m$ values, accumulation of TPP-conjugated compounds in mitochondria can increase up to 100- to 1000-fold, and many tumor cells have larger $\Delta\psi_m$ than their normal counterparts, which facilitates selective accumulation of TPP-linked drugs in tumor cells (13, 17).

A very recent study has demonstrated that, among the TPP-conjugated antioxidants, mitochondria-targeted carboxy-proxyl (Mito-CP) has relatively high efficacy in suppressing proliferation of breast cancer cells (18). In the present study, we evaluate therapeutic potential of Mito-CP for MTC in comparison with vandetanib using in vitro culture models of the human MTC cell lines TT and MZ-CRC-1 and TT xenografts in mice. Furthermore, we investigate the mechanisms underlying the effect of Mito-CP on MTC cells.

Materials and Methods

Cell culture and reagents

The human MTC lines TT and MZ-CRC-1 were maintained as previously described (19–21). Briefly, TT was maintained in RPMI 1640 (Invitrogen, Carlsbad, California) supplemented with 16% fetal bovine serum (FBS), 100 U of penicillin, and 100 μg of streptomycin per milliliter. MZ-CRC-1 was maintained in high-glucose DMEM (Invitrogen) supplemented with 10% FBS in culture dishes coated with rat collagen (Sigma, St. Louis, Missouri). All experiments were performed using cells within 10 passages from the point of acquisition. Cells were seeded at 10^5 cells/mL for the extracellular flux assay and at 2×10^5 cells/mL for all other experiments. The doubling time of TT and MZ-CRC-1 cells were about 70 hours and about 90 hours, respectively. Mito-CP (22) was obtained from Balaraman Kalyanaraman (Medical College of Wisconsin). CP, methyl-TPP, *N*-acetylcysteine (NAC), and tetramethyl-rhodamine ethyl ester perchlorate (TMRE) were purchased from Sigma. 5-(and-6)-Carboxy-2′,7′-dichlorodihydrofluorescein diacetate (carboxy-H_2DCFDA) and vandetanib were purchased from Invitrogen and LC Laboratories (Woburn, Massachusetts), respectively. Z-VAD(OMe)-FMK and Z-D(OMe)QMD(OMe)-FMK were purchased from Millipore (Billerica, Massachusetts).

MTT assay

The colorimetric 3-(4,5-dimethyl-2-thiazolyl)-2,5-diphenyltetrazolium bromide (MTT) (Sigma) assay was performed as previously described (23). Briefly, cells were seeded in 96-well plates and allowed to attach for 48 hours. After drug treatment, cells were incubated with 100 μL of MTT (0.5 mg/mL) in phenol-red–free medium for 2 hours at 37°C, switched into 200 μL of dimethylsulfoxide (DMSO), and shaken for 5 minutes at room temperature before measuring absorbance at 540 nm.

Cell cycle analysis

Cells were washed in ice-cold PBS, fixed in 70% ethanol at −20°C, stained with propidium iodide (50 μg/mL) in 3.8mM sodium citrate/PBS containing ribonuclease A (0.5 mg/mL) for 2 hours on ice, and analyzed by LSR-II flow cytometer (Becton Dickinson, San Jose, California) with a gate that selects single cells within a normal size range. Cell cycle parameters from 20 000 gated cells were determined and analyzed using FCS Express software (De Novo Software, Los Angeles, California).

Detection of mitochondrial membrane potential

Cells were incubated with TMRE (10 ng/mL) in culture medium for 15 minutes at 37°C in the dark, washed with PBS, and switched into phenol-red–free medium before visualizing fluorescence under a microscope. For flow cytometric measurement, TMRE-treated cells were resuspended in 0.1% BSA/PBS and analyzed by flow cytometry (phycoerythrin channel, 575 nm). Data from 20 000 cells were analyzed using FCS Express software.

Detection of oxidative stress

Cells were pretreated with 1μM carboxy-H_2DCFDA in culture medium at 37°C for 1 hour. Cells were then treated with drugs for 2 hours in the dark, trypsinized, resuspended in PBS, and analyzed by flow cytometry (fluorescein isothiocyanate [FITC] channel, 525 nm). Data from 20 000 cells were analyzed using FCS Express software.

Extracellular flux assay

Cells seeded in specialized V3 Seahorse tissue culture plates were treated with Mito-CP for 12 hours. Oxygen consumption rates and extracellular acidification rates were determined using an XF96 Extracellular Flux Analyzer (Seahorse Bioscience, North Billerica, Massachusetts), as previously described (18). Upon completing the measurement, protein concentrations were determined by Bradford assay (Bio-Rad, Hercules, California) to normalize the data.

Immunoblot analysis

Cells were lysed in 62.5mM Tris (pH 6.8)/2% SDS mixed with the protease inhibitor cocktail (Sigma) and briefly sonicated before determining the protein concentration using the bicinchoninic acid reagent (Pierce, Rockford, Illinois). 50 μg of protein was resolved by SDS-PAGE and transferred to a polyvinylidene difluoride membrane filter (Bio-Rad). Membrane filters were blocked in 0.1 M Tris (pH 7.5)/0.9% NaCl/0.05% Tween 20 with 5% nonfat dry milk and incubated with the appropriate antibodies. Antibodies were diluted as follows: ERK1/2, 1:2500; phospho-ERK1/2 (Thr202/Tyr204), 1:2500; glyceraldehyde-3-phosphate dehydrogenase (GAPDH), 1:5000; poly(ADP-ribose) polymerase (PARP), 1:1000; B-cell lymphoma 2 (Bcl-2), 1:2000; B-cell lymphoma-extra large (Bcl-xL), 1:2000 (Cell Signaling Biotechnology, Danvers, Massachusetts); RET, 1:1000 (sc-167, Santa Cruz Biotechnology, Santa Cruz, California); phospho-RET (Tyr1062), 1:1000 (R&D Systems, Minneapolis, Minnesota). The Supersignal West Femto and Pico chemiluminescence kits (Pierce) were used for visualization of the signal. Images of immunoblots were taken and processed using ChemiDoc XRS+ and Image Lab version 3.0 (Bio-Rad).

RT-PCR analysis

RT-PCR was performed by reverse transcription of 0.5 μg total RNA isolated using Trizol (Invitrogen) and the subsequent 25 cycles of PCR using *Taq* polymerase (Invitrogen). For calcitonin, AGTGAGCTGGAGCAGGAGCAAGAG and TCAAATGATCAGCACATTCAGAAG were used. For calcitonin gene-related peptide (CGRP), AGTGAGCTGGAGCAGGAGCAAGAG and CATTACCATGTGTCCCCAGATGCC were used. For RET splicing variant 2 (RET51), ATCCACTGTGCGACGAGC and ACCTTTCACAAAGAAATGTTAACTATC were used. For RET splicing variant 4 (RET9), ATCCACTGTGCGACGAGC and TGCAGAGGGGACAGCGGTGCTAGAA were used. The results were normalized for GAPDH amplified by CGGAGTCAACGGATTTGGTCGTAT and AGCCTTCTCCATGGTGGTGAAGAC.

Tumor xenograft studies

A total of 1×10^7 TT cells in 200 μL HBSS were inoculated sc into the rear flanks of 6-week-old female athymic nude (*nu/nu*) mice (Charles River Laboratories, Wilmington, Massachusetts). Once palpable, tumors were measured using Vernier calipers at intervals indicated in the text. Tumor volumes were calculated using the following formula: length $\times$ width $\times$ height $\times$ 0.5236. When tumor volumes reached 100 mm^3, mice were sorted into 3 groups of 6 to achieve equal distribution of tumor size in all treatment groups. Group 1 received only the vehicle (1:9 mixture of DMSO/Cremophore-EL; Sigma), group 2 received Mito-CP (40 mg/kg body weight per dose), and group 3 received vandetanib (40 mg/kg body weight per dose). Mito-CP and vandetanib dissolved in 200 μL vehicle were orally administered by gavage every 2 days (total 10 doses). At the end of the experiment, animals were euthanized by CO_2 asphyxiation. All animal studies were performed according to protocols approved by the Institutional Animal Care and Use Committee at Medical College of Wisconsin.

Statistical analysis

Two-tailed unpaired Student's *t* test was used to assess the statistical significance of 2 data sets. The significance of tumor xenograft studies was determined by 1-way ANOVA with Bonferroni correction for multiple comparisons. P value $< .05$ was considered statistically significant.

Results

Mitochondrial-specific targeting of Mito-CP induces growth-inhibitory effects in MTC cells

Mito-CP consists of the CP moiety, a 5-membered nitroxide that has antioxidant properties, and the TPP moiety that mediates mitochondria targeting; chemical structures of Mito-CP and its control compounds are depicted in Figure 1 of Ref. 24. We determined whether Mito-CP can induce growth-inhibitory effects in TT and MZ-CRC-1, which are the most thoroughly characterized human MTC lines and, thus, have been extensively used for evaluation of different therapeutic agents (25–27). As a control to validate mitochondrial-specific effects of Mito-CP, we also examined the 2 individual functional moieties of Mito-CP, CP, and TPP. When determined by MTT assay, Mito-CP treatment in 0.01μM to 25μM dose ranges for 48 hours could significantly decrease cell viability of these cells, with TT exhibiting slightly higher sensitivity than MZ-CRC-1 (Figure 1A); IC_{50} values were calculated at 0.38μM for TT and 0.89μM for MZ-CRC-1. In contrast, equal doses of the antioxidant moiety, CP, or the mitochondrial carrier, TPP, did not significantly affect the growth of these cells except that TPP decreased TT cell viability at higher doses, albeit less significantly than Mito-CP (Figure 1A).

To determine by what mechanism Mito-CP suppressed MTC cell growth, we conducted cell cycle analysis and found that Mito-CP treatment effectively induced cell death in the MTC cells, as indicated by the dose-dependent accumulation of cell population in the sub-G0/G1 phase (Figure 1B, additional data shown below). These data in-

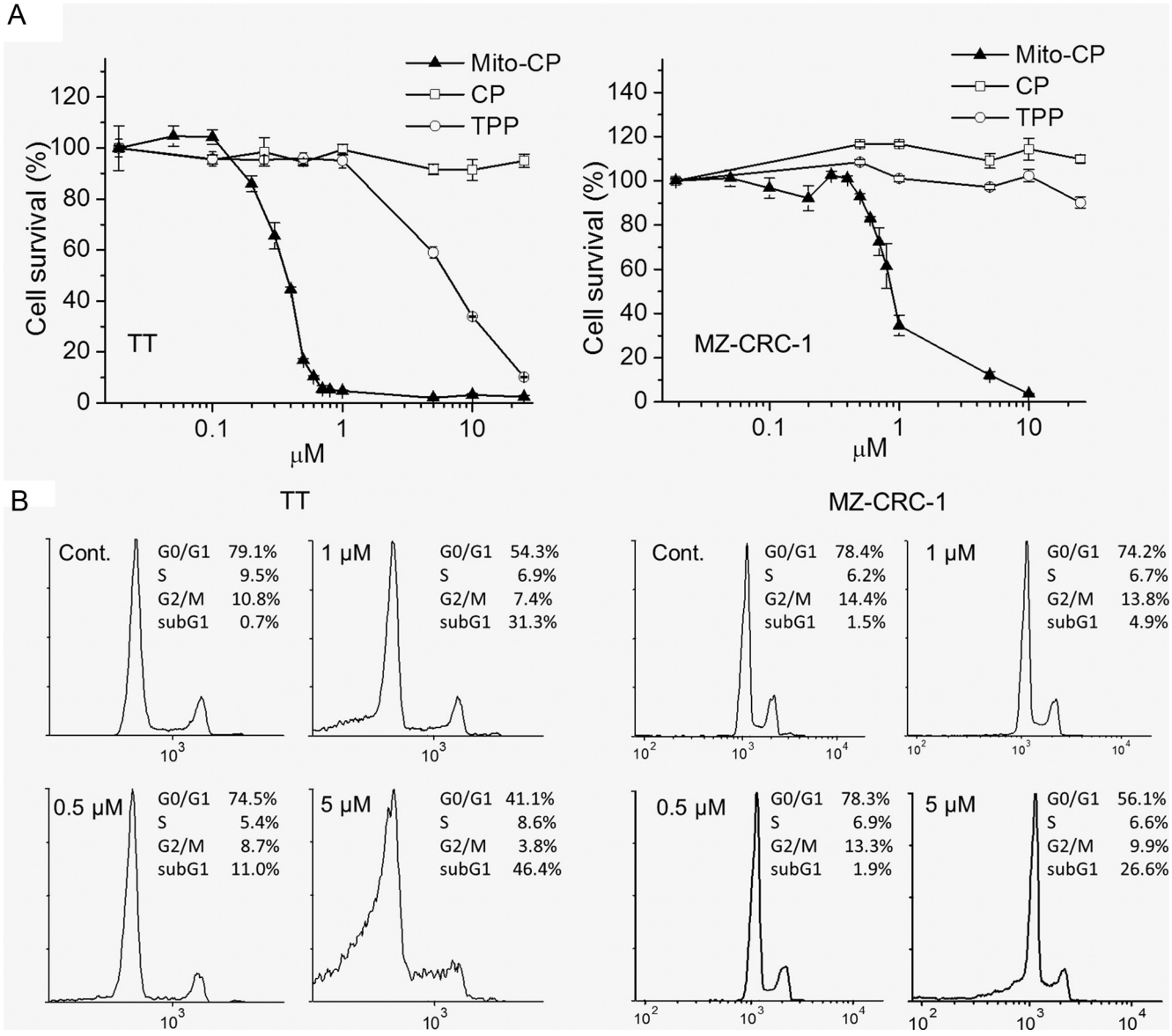

Figure 1. Mito-CP is cytotoxic in MTC cells. A, TT and MZ-CRC-1 cells in 96-well plates were treated with serially increasing doses of Mito-CP or the control (Cont) compounds for 48 hours. Chemical structure of Mito-CP and its control compounds were previously shown (24). Cells were then allowed to recover in drug-free fresh medium for 48 hours before the measurement of cell viability by MTT assay. Data (mean ± SD, n = 6) are expressed as the percentage of untreated control. B, TT and MZ-CRC-1 cells were treated with Mito-CP at the indicated doses for 24 hours before cell cycle analysis using propidium iodide. Control cells were treated with an equal volume of DMSO.

dicate that mitochondrial-specific delivery of CP can effectively suppress MTC cell growth by inducing cytotoxic effects.

The in vitro efficacy of Mito-CP is comparable to vandetanib, and Mito-CP induces RET downregulation and caspase-dependent apoptosis contrary to vandetanib

We next assessed Mito-CP for its efficacy relative to vandetanib in suppressing MTC cells. When treated with these drugs at different doses for 48 hours, TT and MZ-CRC-1 cells exhibited commensurable sensitivity to Mito-CP and vandetanib, with similar IC_{50} ranges being detected for both compounds (Figure 2A). Intriguingly, in the effective dose ranges, Mito-CP induced very steep changes in cellular sensitivity relative to vandetanib in both TT and MZ-CRC-1 cells. This sharp threshold for drug efficacy suggests that Mito-CP may suppress MTC cells via a specific mechanism. These data demonstrate that Mito-CP is similarly effective as vandetanib in suppressing MTC cell growth in vitro.

TT contains RET^{C634W} mutation in the extracellular domain, whereas MZ-CRC-1 has RET^{M918T} mutation in the kinase domain. Western blot analysis revealed that Mito-CP treatment induced substantial RET downregulation in TT and MZ-CRC-1 cells, whereas vandetanib,

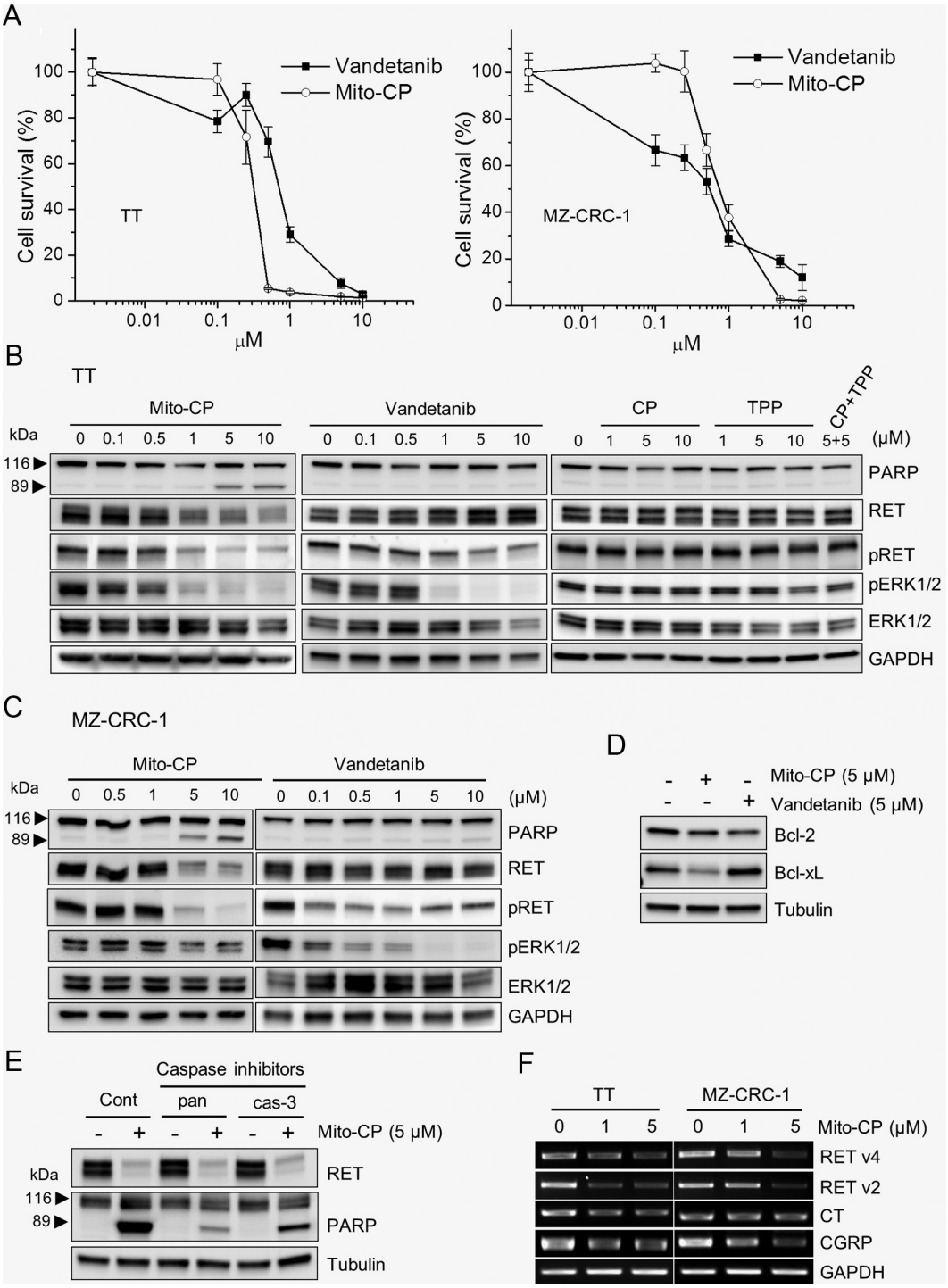

Figure 2. Mito-CP induces RET downregulation and PARP cleavage in MTC cells. A, TT and MZ-CRC-1 cells were treated with different doses of Mito-CP or vandetanib for 48 hours. Cells were then allowed to recover in drug-free fresh medium for 48 hours before the measurement of cell viability by MTT assay. Data (mean ± SD, n = 6) are expressed as the percentage of untreated control. B, Total lysates of TT cells treated with different doses of Mito-CP, vandetanib, or the control compounds for 24 hours were analyzed by Western blotting for PARP cleavage and expression of RET, phosphorylated RET at Tyr1062 (pRET), phosphorylated ERK1/2 (pERK1/2), and ERK1/2. GAPDH is a loading control. C, Total lysates of MZ-CRC-1 cells treated with different doses of Mito-CP or the control compounds for 24 hours were examined by Western blot analysis for expression of the indicated proteins. D, Total lysates of TT cells treated with 5μM Mito-CP and vandetanib for 24 hours were examined by Western blotting for expression of Bcl-2 and Bcl-xL. β-Tubulin is a loading control. E, TT cells were treated with 5μM Mito-CP in the presence of 20μM Z-VAD(OMe)-FMK (pan-caspase inhibitor) or 20μM Z-D(OMe)QMD(OMe)-FMK (caspase-3 inhibitor) for 24 hours. Total lysates were analyzed for RET expression and PARP cleavage. F, Total RNA of TT and MZ-CRC-1 cells treated with Mito-CP for 24 hours were examined by RT-PCR for expression of RET and calcitonin splicing variants CT and CGRP. GAPDH was detected to validate the use of equal amount of RNA samples.

CP, or TPP of equal doses could not induce any similar effects (Figure 2, B and C), indicating the specificity of Mito-CP. Correlated with these effects, Mito-CP also substantially downregulated phosphorylated RET at Tyr1062, a key residue required for RET signaling toward different pathways (5), to the level comparable to vandetanib effects (Figure 2, B and C). Moreover, Mito-CP significantly decreased phosphorylation of ERK1/2, a downstream effector of RET (5), in TT (Figure 2B) and, to a lesser extent, in MZ-CRC-1 (Figure 2C). These data suggest that Mito-CP can effectively deplete RET mutants and suppress RET signaling in MTC cells.

Importantly, in a strong correlation with RET downregulation, Mito-CP, but not CP or TPP, increased the cleavage of PARP in TT and MZ-CRC-1 cells (Figure 2, B and C), which is a signature of caspase-dependent apoptotic cell death (28). When determined in TT cells, Mito-CP downregulated antiapoptotic proteins Bcl-2 and Bcl-xL (Figure 2D). Moreover, both pan-caspase inhibitor and caspase-3 inhibitor significantly blocked PARP cleavage under Mito-CP–treated conditions (Figure 2E). These data are consistent with the increases in sub-G0/G1 phase populations in Mito-CP–treated cultures (Figure 1B), suggesting that Mito-CP induces cell death by activating caspase-dependent apoptotic pathways. By contrast, vandetanib induced neither PARP cleavage nor downregulation of Bcl-xL, although it mildly downregulated Bcl-2, which is consistent with a previous study demonstrating that vandetanib effects are mainly cytostatic in MTC (29). These effects of Mito-CP and vandetanib are in stark contrast and strongly suggest that Mito-CP can suppress MTC cell growth/survival via distinct mechanisms.

Because RET is known as a caspase target (30), we determined whether Mito-CP–induced RET downregulation could be blocked by different caspase inhibitors. Under Mito-CP–treated conditions, both pan-caspase inhibitor and caspase-3 inhibitor could not block RET downregulation, although they significantly blocked PARP cleavage (Figure 2E). Therefore, Mito-CP may regulate RET independently of caspase activity. Next, using RT-PCR techniques, we determined whether Mito-CP affects expression of RET splicing variants 2 (RET51) and 4 (RET9). Mito-CP downregulated mRNA levels of both RET variants in a dose-dependent manner (Figure 2F), indicating that Mito-CP regulates RET at mRNA levels.

In TT and MZ-CRC-1 cells, Mito-CP also downregulated mRNA levels of calcitonin and its splicing variant, CGRP (Figure 2F). However, Mito-CP did not affect cellular levels of human achaete-scute homolog-1 or neuron-specific enolase (Supplemental Figure 1, published on The Endocrine Society's Journals Online web site at http://jcem.endojournals.org), suggesting that Mito-CP may not induce MTC differentiation.

Mito-CP disrupts mitochondrial activity and induces oxidative stress in MTC cells

Only Mito-CP, but not CP or TPP, was effective in suppressing MTC cell survival (Figure 1). Because this implicated mitochondrial damages in the cytotoxic Mito-CP effects on MTC cells, we determined whether Mito-CP disrupts mitochondrial integrity in MTC cells. For that, we examined Mito-CP effects on $\Delta\psi_m$, oxidative stress, and oxygen consumption rates.

When treated with Mito-CP (higher than 5μM) for 2 hours and stained with TMRE, a $\Delta\psi_m$-dependent mitochondrial dye, TT cells exhibited a significant loss of $\Delta\psi_m$ (Figure 3, A and B), which was consistent with the cytotoxic effects detected in the dose range (Figures 1A and 2). These effects were specific to Mito-CP because CP or TPP could not induce any similar changes (Figure 3A). Because loss of mitochondrial integrity is often associated with oxidative stress, we next determined whether Mito-CP treatment could also affect the oxidation levels of carboxy-H_2DCFDA, a redox-sensitive dye that fluoresces upon oxidation (31). In TT and MZ-CRC-1 cells treated with Mito-CP for 2 hours, significantly increased fluorescence of carboxy-H_2DCFDA was detected (Figure 3C), which was even higher than the levels induced by 100μM H_2O_2 (shown in Figure 4A). Moreover, in a dose-dependent manner, Mito-CP treatment for 12 hours significantly decreased oxygen consumption rates and mildly increased extracellular acidification rates in TT and MZ-CRC-1 cells (Figure 3, D and E), suggesting that Mito-CP may alter mitochondrial activity and, possibly, cellular bioenergetics. These data demonstrate the capability of Mito-CP to interfere with mitochondrial function and to induce oxidative stress in MTC cells, implicating mitochondrial damages in its growth-inhibitory effects on MTC cells.

Mito-CP–induced cell death, but not RET downregulation, is partially abrogated by the ROS scavenger NAC

Higher levels of oxidative stress can induce cytotoxic or cytostatic effects in cells, whereas lower levels of the stress can facilitate cell proliferation and differentiation (32). Accordingly, we determined the significance of Mito-CP–induced oxidative stress in MTC cells, using the cell-permeable ROS scavenger NAC.

Pretreatment of TT cells with 5mM NAC could consistently, albeit modestly, reduce the levels of carboxy-

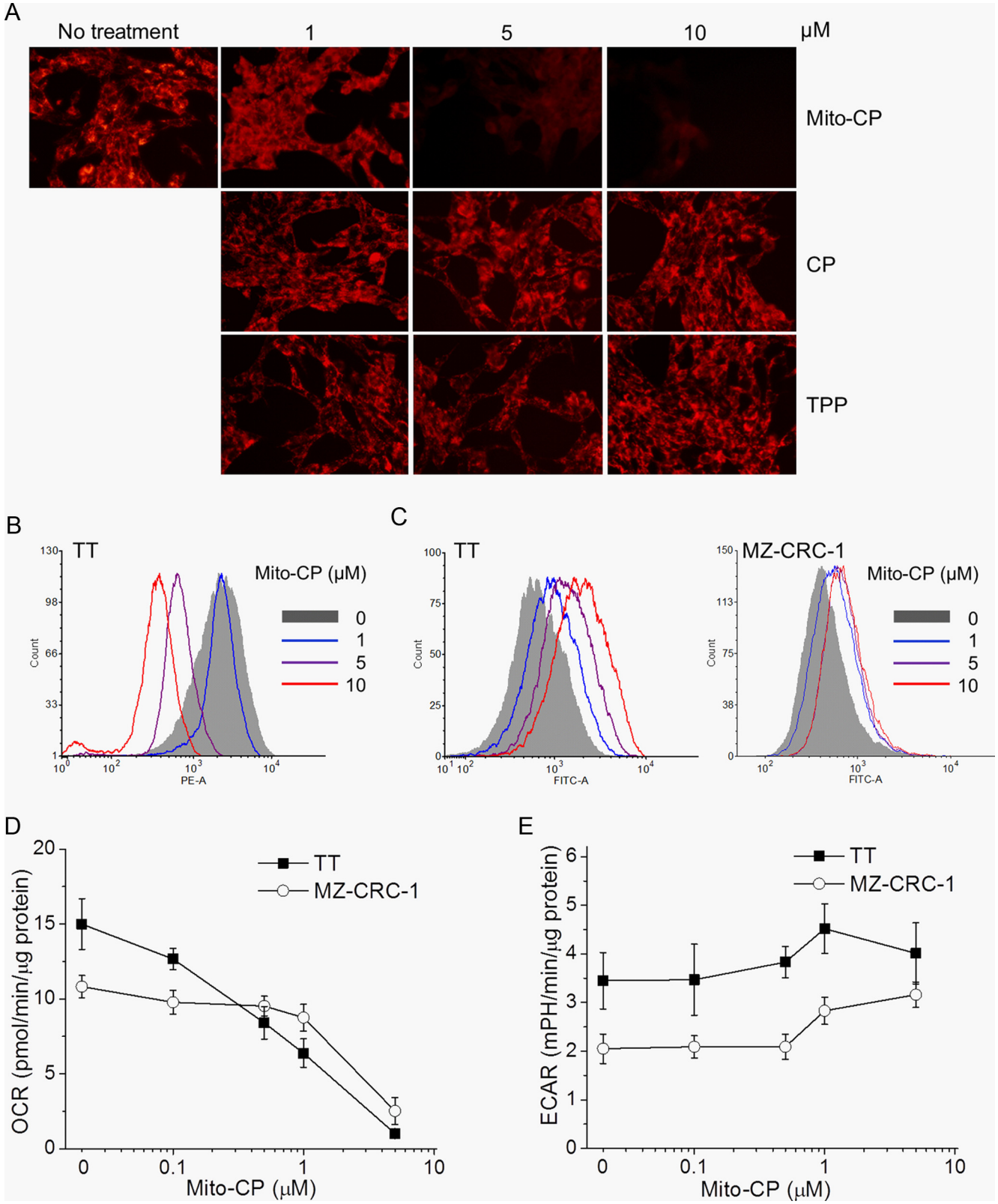

Figure 3. Mito-CP induces loss of mitochondrial membrane potential, upregulates ROS generation, and decreases oxygen consumption in MTC cells. A, TT cells, treated with Mito-CP or control compounds for 2 hours, were stained with TMRE. Changes in the mitochondrial membrane potential were then visualized under a fluorescent microscope (magnification, ×40). B, TT cells, treated with Mito-CP and stained with TMRE, were analyzed by flow cytometry to measure red fluorescence (phycoerythrin channel, 575 nm). C, TT and MZ-CRC-1 cells, pretreated with 1μM carboxy-H_2DCFDA for 1 hour, were treated with Mito-CP in a dye-free culture medium. Cells were harvested and analyzed by flow cytometry to measure green fluorescence (FITC channel, 525 nm). D and E, Oxygen consumption rates (OCR) and extracellular acidification rates (ECAR) in TT and MZ-CRC-1 cells treated with indicated doses of Mito-CP for 12 hours were measured as described in Materials and Methods. Data (mean ± SD, n = 6) are normalized to protein amounts in cell culture.

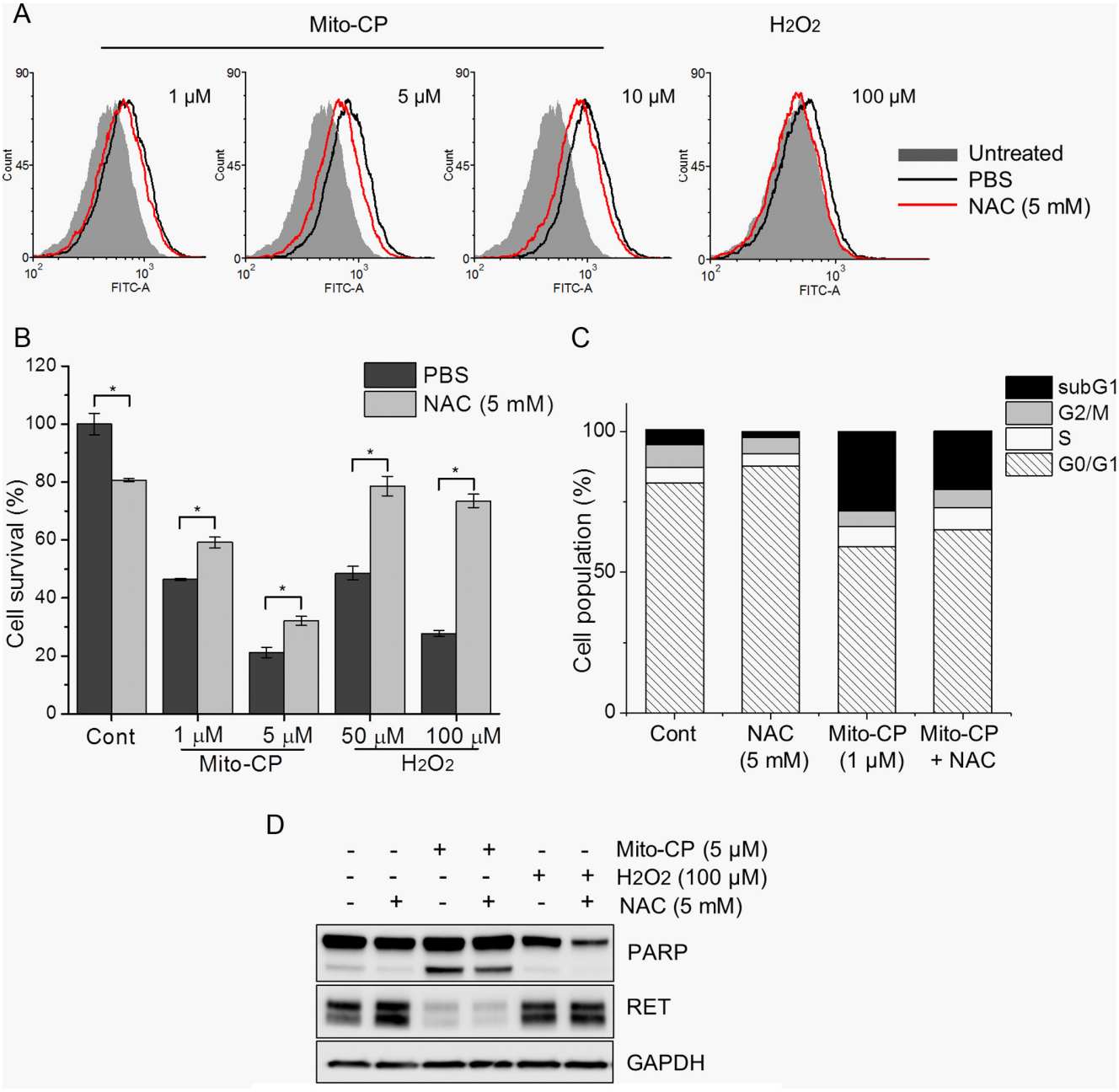

Figure 4. The ROS scavenger NAC partially attenuates Mito-CP–induced cell death, but not RET downregulation, in TT cells. A, Cells were pretreated with 5mM NAC for 24 hours, incubated with 1μM carboxy-H_2DCFDA for 1 hour, and then treated with Mito-CP at the indicated doses for 2 hours before flow cytometry (FITC channel, 545 nm). H_2O_2 was used as the control. B, Cells pretreated with 5mM NAC for 24 hours were treated with Mito-CP or H_2O_2 at the indicated doses in the medium containing 2% FBS for 24 hours. Cell viability was determined by MTT assay. Data (mean ± SD, n = 4) are expressed as the percentage of untreated control; *$P < .0001$, *t* test. C, TT cells were treated with 1μM Mito-CP in the presence or absence of 5mM NAC for 24 hours before cell cycle analysis. Control cells were treated with an equal volume of vehicle. D, Cells were treated with 5μM Mito-CP or 100μM H_2O_2 in the presence of 5mM NAC in the medium containing 2% FBS for 24 hours. Total cell lysates were analyzed by Western blotting for RET expression and PARP cleavage. GAPDH is a loading control.

H_2DCFDA fluorescence under different Mito-CP treatment conditions (Figure 4A). Consistent with this, NAC pretreatment partially rescued cells from Mito-CP toxicity, as determined by MTT assay (Figure 4B), by measuring sub-G0/G1 phase population (Figure 4C) and by Western blot analysis of PARP cleavage (Figure 4D). However, NAC pretreatment did not attenuate Mito-CP–induced RET downregulation (Figure 4D), suggesting that Mito-CP also mediates a mechanism independent of oxidative stress to suppress TT cell growth. In support of this notion, despite exhibiting comparable cytotoxicity (Figure 4B), H_2O_2 did not affect RET or PARP protein levels in TT cells (Figure 4D). Therefore, Mito-CP appears to mediate growth inhibition in MTC cells partly by inducing oxidative stress and partly by mediating other mechanisms.

Mito-CP effectively suppresses growth of TT xenografts in mice

Lastly, we evaluated the potential of Mito-CP to suppress MTC using a TT xenograft model in immune-compromised nude mice according to the treatment schedule previously used to extrapolate the human pharmacokinetics of vandetanib in mice (33).

Consistent with the in vitro data above, oral administration of Mito-CP effectively suppressed the growth of TT xenografts in mice throughout the treatment (Figure 5, A and B) and induced RET downregulation, PARP cleavage, and downregulation of Bcl-xL and Bcl-2 in the tumor (Figure 5C). However, analysis of hematoxylin- and eosin-stained tumor resections did not reveal any indication

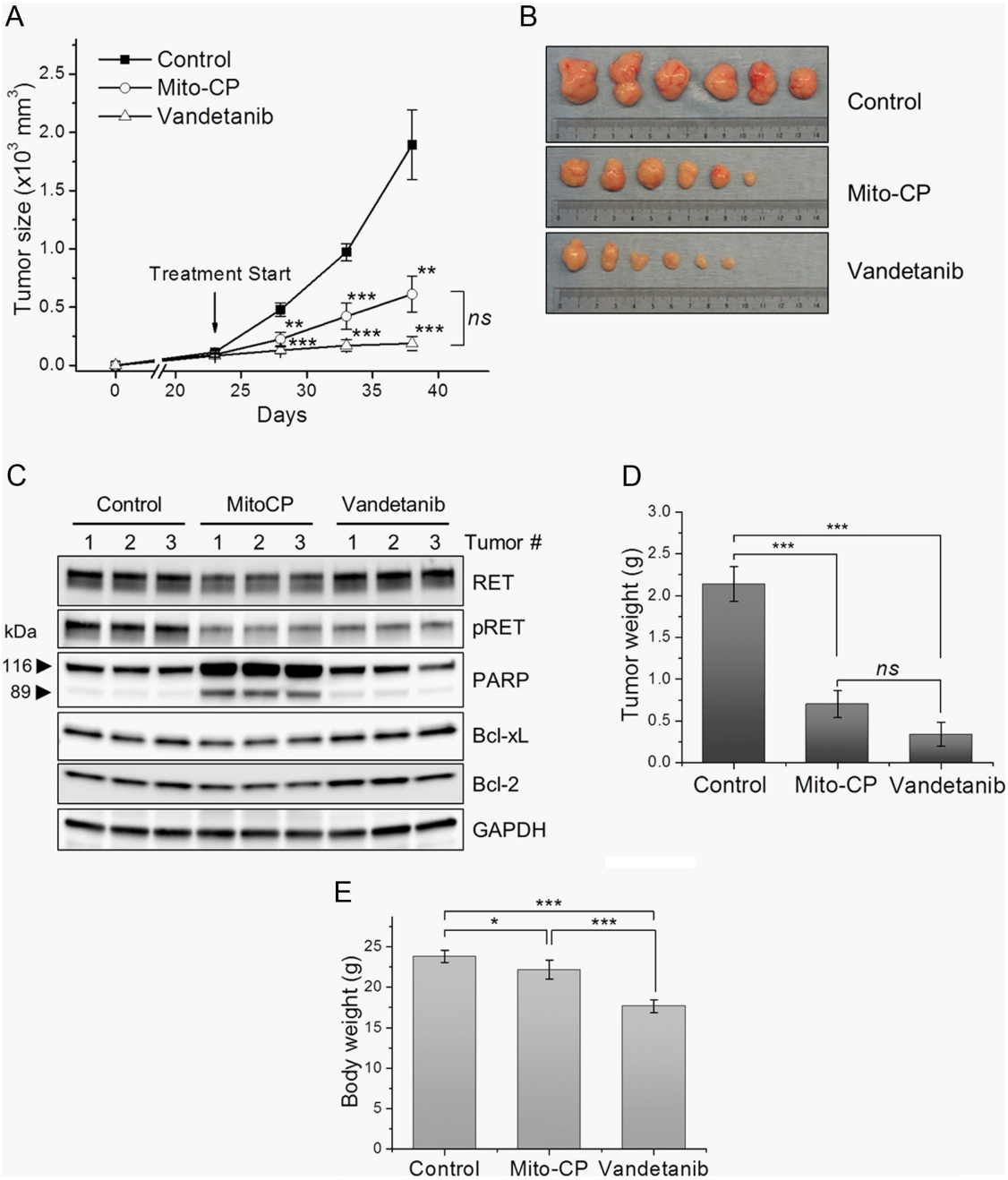

Figure 5. Mito-CP suppresses TT xenografts in athymic mice. Athymic mice bearing TT xenografts were treated with 10 doses of Mito-CP and vandetanib (40 mg/kg/dose). Drugs were administered per os every 2 days beginning from day 23 after tumor implantation. The control group was treated with the vehicle only (details in Materials and Methods). A, Changes in tumor sizes were determined at the indicated time points. B, Images of tumors collected at the end of the treatment. C, Homogenates of 3 tumor xenografts from each group were analyzed by Western blotting for expression of indicated proteins. D, Weights of tumors collected at the end of the treatment. E, Body weights of animals at the end of treatment. All data are mean ± SEM (n = 6). *$P < .05$; **$P < .01$; ***$P < .001$; ns, not significant ($P > .05$), 1-way ANOVA with Bonferroni correction for multiple comparisons.

of necrosis (Supplemental Figure 2). Of note, although TPP-conjugated compounds are known to be distributed to mitochondria in all organs, including the brain (34), the dosage of Mito-CP in this experiment did not affect RET levels in the brain (Supplemental Figure 3).

When tumor weights were measured at the end of the treatment, about 67% and 84% decreases relative to the vehicle-treated control were detected in Mito-CP–treated and vandetanib-treated groups, respectively (Figure 5D). Importantly, although Mito-CP and vandetanib, administered at equivalent doses, induced similar tumor-suppressive effects in this experiment, Mito-CP-treated mice exhibited less than 5% decreases in body weight, whereas vandetanib-treated group showed about 25% decreases (Figure 5E), suggesting that Mito-CP was better tolerated with less systemic toxicity in mice. Therefore, although Mito-CP and vandetanib may be controlled by different pharmacokinetics in vivo, it appears that Mito-CP treatment can be further optimized. These findings strongly support the therapeutic potential of Mito-CP for MTC treatment.

Discussion

MTC is generally not responsive to classic chemotherapy or radiation therapy. Therefore, extensive surgical resection of thyroid and lymph nodes is currently the only curative treatment, although not effective for metastatic or recurring MTC (1). Vandetanib treatment has been shown to be effective in about 50% of the progressive MTC cases (6, 8), requiring the development of a therapeutic strategy for those unresponsive patients. This study demonstrates that Mito-CP may have a potential to meet this demand because of its distinct effects. Contrary to vandetanib, Mito-CP induced RET downregulation and strong cytotoxic effects. Given that RET is a key etiological factor for MTC and that cytotoxicity is a more desirable effect of a cancer drug than cytostasis, our findings have potential clinical significance.

The efficacy of Mito-CP in MTC cells suggests that the mitochondria may be a novel therapeutic target for MTC treatment. Mitochondria are the key intracellular organelle responsible for the generation of ATP and certain building blocks, for which a series of enzymes in the respiratory chain and the citric acid cycle are required. The aerobic glycolysis detected in different cancer cells, the so-called Warburg effect, initially led to various hypotheses that underestimate the significance of mitochondrial metabolism in cancer (reviewed in Refs. 9 and 35). However, it is now appreciated that reprogrammed mitochondrial metabolism in cancer facilitates tumor cell proliferation and survival. Indeed, mitochondrial oxidative phosphorylation is critical in cancer to meet increased demands for the production of building blocks and energy required for uncontrolled tumor cell proliferation, as demonstrated in many different cell lines, derived from malignant tumors of bone, lung, breast, skin, cervix, ovary, and uterus (36–38). Currently, the information on mitochondrial alterations in MTC is very limited, and better understanding in this regard is necessary to further evaluate the potential of mitochondria as a therapeutic target in MTC.

Therapeutic effects of TPP-linked drugs are attributed to their specific enrichment in the mitochondria. Nevertheless, it is yet unclear how Mito-CP mediates tumor-suppressive effects without seriously damaging normal cells. It was previously reported that many tumor cells have a more negative mitochondrial membrane potential than their normal counterparts, which may account for selective accumulation of TPP-linked drugs in the mitochondria of tumor cells (13, 17). In support, Mito-CP was previously shown to inhibit proliferation of the breast cancer cell lines MCF-7 and MDA-MB-231 but not the normal MCF-10A cells (18, 24). The lack of a normal thyroid C-cell control did not allow a similar evaluation in this study. Nevertheless, it is evident that Mito-CP was not highly toxic to mice despite its negative effects on the MTC xenografts.

Given that Mito-CP induces an effect to disrupt mitochondrial integrity, it may be conceivable that oxidative damages associated with the dysfunctional mitochondria partly underlie MTC cell casualty. The increased carboxy-H_2DCFDA fluorescence suggests onset of oxidative stress, which may include increased ROS generation as well as other aberrant redox modifications in cells (31). ROS is a major cause for oxidative stress in cells, and our NAC treatment data supports the possibility that increased ROS may partly mediate Mito-CP effects in MTC cells. However, increased ROS generation would be a paradoxical effect of Mito-CP given the chemical property of nitroxide as an antioxidant (39). Mitochondria-targeted antioxidants can effectively protect cells from oxidative damage under different pathophysiological conditions by scavenging ROS generated at different segments of the mitochondrial respiratory chain (15). Consistent with this, Mito-CP could protect normal bovine aortic endothelial cells from peroxide-induced stress (22). Nevertheless, the exact mechanisms of Mito-CP effects in different cell types are yet unclear, whereas increased ROS generation is not a totally unusual effect of a chemical with antioxidant property. For example, the well-known antioxidant vitamin C can mediate strong pro-oxidant effects by inducing the Fenton reaction in cells depending upon the balance be-

tween its concentration and the availability of catalytic metal ions, which may be varied in different cell contexts (40). Furthermore, high-dose vitamin C was considered for cancer therapy based upon its capability to increase ROS levels and oxidative damages in certain tumor cells (40). Therefore, it may be possible that Mito-CP induces MTC suppression in a similar context. On the other hand, Mito-CP inhibited oxygen consumption and slightly increased extracellular acidification in MTC cultures, which is indicative of the blockage of oxidative phosphorylation. These effects of Mito-CP are consistent with its effects in breast cancer cells (18) and may contribute to the generation of superoxide radicals via electron leakage.

Of note, given the inability of NAC and H_2O_2 to affect RET, Mito-CP may mediate RET downregulation independently of oxidative stress. Furthermore, the known caspase-dependent mechanism (30) does not seem to be involved. Therefore, it appears that Mito-CP–mediated mitochondrial targeting triggers multiple mechanisms to suppress MTC, including redox-dependent and -independent as well as caspase-dependent and -independent mechanisms. Because our data indicate that Mito-CP regulates RET at mRNA levels, it is interesting to ask what specific mechanisms in the mitochondria are activated by Mito-CP to regulate RET. Further investigation in this regard is warranted.

Recent clinical studies reported that vandetanib treatment is usually accompanied by grade 3 or higher adverse effects, including abdominal pain and diarrhea, rashes, hypertension, headache, and fatigue (6, 8). Therefore, a strategy is required to reduce the toxicity of vandetanib without compromising therapeutic effects. The distinct effects of Mito-CP relative to vandetanib may allow a combinatory treatment using both agents. If possible, this strategy would reduce the effective dosage of vandetanib and, accordingly, its toxicity. In conclusion, our results strongly support the potential of Mito-CP for MTC treatment.

Acknowledgments

We thank Dr Robert Gagel for MZ-CRC-1, Drs Balaraman Kalyanaraman and Joy Joseph for Mito-CP, Steven Komas and Dr Brian Dranka for Seahorse analysis, and Dr Sergey Tarima for statistical analysis.

Address all correspondence and requests for reprints to: Jong-In Park, PhD, Department of Biochemistry, Medical College of Wisconsin, 8701 Watertown Plank Road, Milwaukee, Wisconsin 53226. E-mail: jipark@mcw.edu.

This work was supported by the American Cancer Society (RSGM-10-189-01-TBE), National Institutes of Health (1R01CA138441), and Flight Attendant Medical Research Institute Young Investigator Award (062438) to J.P., and partly by the Medical College of Wisconsin Cancer Center Bioenergetics shared resource.

Disclosure Summary: The authors have nothing to declare.

References

1. **Tuttle RM, Ball DW, Byrd D, et al.** Medullary carcinoma. *J Natl Compr Canc Netw*. 2010;8:512–530.
2. **Agrawal N, Jiao Y, Sausen M, et al.** 2012 Exomic sequencing of medullary thyroid cancer reveals dominant and mutually exclusive oncogenic mutations in RET and RAS. *J Clin Endocrinol Metab*. 2013;98:E364–E369.
3. **Boichard A, Croux L, Al Ghuzlan A, et al.** Somatic RAS mutations occur in a large proportion of sporadic RET-negative medullary thyroid carcinomas and extend to a previously unidentified exon. *J Clin Endocrinol Metab*. 2012;97:E2031–E2035.
4. **Ciampi R, Mian C, Fugazzola L, et al.** Evidence of a low prevalence of RAS mutations in a large medullary thyroid cancer series. *Thyroid*. 2013;1:1–8.
5. **Ichihara M, Murakumo Y, Takahashi M.** RET and neuroendocrine tumors. *Cancer Lett*. 2004;204:197–211.
6. **Degrauwe N, Sosa JA, Roman S, Deshpande HA.** Vandetanib for the treatment of metastatic medullary thyroid cancer. *Clin Med Insights Oncol*. 2012;6:243–252.
7. **Nagilla M, Brown RL, Cohen EE.** Cabozantinib for the treatment of advanced medullary thyroid cancer. *Adv Ther*. 2012;29:925–934.
8. **Wells SA Jr, Robinson BG, Gagel RF, et al.** Vandetanib in patients with locally advanced or metastatic medullary thyroid cancer: a randomized, double-blind phase III trial. *J Clin Oncol*. 2012;30:134–141.
9. **Ward PS, Thompson CB.** Metabolic reprogramming: a cancer hallmark even Warburg did not anticipate. *Cancer Cell*. 2012;21:297–308.
10. **Chiarugi P, Fiaschi T.** Redox signalling in anchorage-dependent cell growth. *Cell Signal*. 2007;19:672–682.
11. **Rao VA, Klein SR, Bonar SJ, et al.** The antioxidant transcription factor Nrf2 negatively regulates autophagy and growth arrest induced by the anticancer redox agent mitoquinone. *J Biol Chem*. 2010;285:34447–34459.
12. **Weinberg F, Hamanaka R, Wheaton WW, et al.** Mitochondrial metabolism and ROS generation are essential for Kras-mediated tumorigenicity. *Proc Natl Acad Sci U S A*. 2010;107:8788–8793.
13. **Don AS, Hogg PJ.** Mitochondria as cancer drug targets. *Trends Mol Med*. 2004;10:372–378.
14. **Millard M, Pathania D, Shabaik Y, Taheri L, Deng J, Neamati N.** 2010 Preclinical evaluation of novel triphenylphosphonium salts with broad-spectrum activity. *PloS one*. 5:pii:e13131.
15. **Murphy MP, Smith RA.** Targeting antioxidants to mitochondria by conjugation to lipophilic cations. *Annu Rev Pharmacol Toxicol*. 2007;47:629–656.
16. **Smith RA, Adlam VJ, Blaikie FH, et al.** Mitochondria-targeted antioxidants in the treatment of disease. *Ann N Y Acad Sci*. 2008;1147:105–111.
17. **Modica-Napolitano JS, Aprille JR.** Delocalized lipophilic cations selectively target the mitochondria of carcinoma cells. *Adv Drug Deliv Rev*. 2001;49:63–70.
18. **Cheng G, Zielonka J, Dranka BP, et al.** Mitochondria-targeted drugs synergize with 2-deoxyglucose to trigger breast cancer cell death. *Cancer Res*. 2012;72:2634–2644.
19. **Arthan D, Hong SK, Park JI.** Leukemia inhibitory factor can mediate Ras/Raf/MEK/ERK-induced growth inhibitory signaling in medullary thyroid cancer cells. *Cancer Lett*. 2010;297:31–41.
20. **Park JI, Strock CJ, Ball DW, Nelkin BD.** The Ras/Raf/MEK/extracellular signal-regulated kinase pathway induces autocrine-para-

crine growth inhibition via the leukemia inhibitory factor/JAK/STAT pathway. *Mol Cell Biol*. 2003;23:543–554.
21. **Park JI, Strock CJ, Ball DW, Nelkin BD.** Interleukin-1β can mediate growth arrest and differentiation via the leukemia inhibitory factor/JAK/STAT pathway in medullary thyroid carcinoma cells. *Cytokine*. 2005;29:125–134.
22. **Dhanasekaran A, Kotamraju S, Karunakaran C, et al.** Mitochondria superoxide dismutase mimetic inhibits peroxide-induced oxidative damage and apoptosis: role of mitochondrial superoxide. *Free Radic Biol Med*. 2005;39:567–583.
23. **Hong SK, Yoon S, Moelling C, Arthan D, Park JI.** Noncatalytic function of ERK1/2 can promote Raf/MEK/ERK-mediated growth arrest signaling. *J Biol Chem*. 2009;284:33006–33018.
24. **Cheng G, Lopez M, Zielonka J, et al.** Mitochondria-targeted nitroxides exacerbate fluvastatin-mediated cytostatic and cytotoxic effects in breast cancer cells. *Cancer Biol Ther*. 2011;12:707–717.
25. **de Groot JW, Plaza Menacho I, Schepers H, et al.** Cellular effects of imatinib on medullary thyroid cancer cells harboring multiple endocrine neoplasia type 2A and 2B associated RET mutations. *Surgery*. 2006;139:806–814.
26. **Morisi R, Celano M, Tosi E, et al.** 2007 Growth inhibition of medullary thyroid carcinoma cells by pyrazolo-pyrimidine derivates. *J Endocrinol Invest*. 30:RC31–RC34.
27. **Plaza-Menacho I, Mologni L, Sala E, et al.** Sorafenib functions to potently suppress RET tyrosine kinase activity by direct enzymatic inhibition and promoting RET lysosomal degradation independent of proteasomal targeting. *J Biol Chem*. 2007;282:29230–29240.
28. **Rosen A, Casciola-Rosen L.** Macromolecular substrates for the ICE-like proteases during apoptosis. *J Cell Biochem*. 1997;64:50–54.
29. **Vitagliano D, De Falco V, Tamburrino A, et al.** The tyrosine kinase inhibitor ZD6474 blocks proliferation of RET mutant medullary thyroid carcinoma cells. *Endocr Relat Cancer*. 2011;18:1–11.
30. **Cabrera JR, Bouzas-Rodriguez J, Tauszig-Delamasure S, Mehlen P.** RET modulates cell adhesion via its cleavage by caspase in sympathetic neurons. *J Biol Chem*. 2011;286:14628–14638.
31. **Kalyanaraman B, Darley-Usmar V, Davies KJ, et al.** Measuring reactive oxygen and nitrogen species with fluorescent probes: challenges and limitations. *Free Radic Biol Med*. 2012;52:1–6.
32. **Halliwell B.** Oxidative stress and cancer: have we moved forward? *Biochem J*. 2007;401:1–11.
33. **Gustafson DL, Bradshaw-Pierce EL, Merz AL, Zirrolli JA.** Tissue distribution and metabolism of the tyrosine kinase inhibitor ZD6474 (Zactima) in tumor-bearing nude mice following oral dosing. *J Pharmacol Exp Ther*. 2006;318:872–880.
34. **Smith RA, Porteous CM, Gane AM, Murphy MP.** Delivery of bioactive molecules to mitochondria in vivo. *Proc Natl Acad Sci U S A*. 2003;100:5407–5412.
35. **Chen Z, Lu W, Garcia-Prieto C, Huang P.** The Warburg effect and its cancer therapeutic implications. *J Bioenerg Biomembr*. 2007;39:267–274.
36. **Balaban RS, Bader JP.** Studies on the relationship between glycolysis and $(Na^+ + K^+)$-ATPase in cultured cells. *Biochim Biophys Acta*. 1984;804:419–426.
37. **Chen ZX, Velaithan R, Pervaiz S.** mitoEnergetics and cancer cell fate. *Biochim Biophys Acta*. 2009;1787:462–467.
38. **Kallinowski F, Schlenger KH, Kloes M, Stohrer M, Vaupel P.** Tumor blood flow: the principal modulator of oxidative and glycolytic metabolism, and of the metabolic micromilieu of human tumor xenografts in vivo. *Int J Cancer*. 1989;44:266–272.
39. **Krishna MC, Russo A, Mitchell JB, Goldstein S, Dafni H, Samuni A.** Do nitroxide antioxidants act as scavengers of $O_2^{-\cdot}$ or as SOD mimics? *J Biol Chem*. 1996;271:26026–26031.
40. **Du J, Cullen JJ, Buettner GR.** Ascorbic acid: chemistry, biology and the treatment of cancer. *Biochim Biophys Acta*. 2012;1826:443–457.